Relationship between Stress and Dangling Bond Generation at the (111)Si/SiO2 Interface

A. Stesmans

Physics Department, Universiteit Leuven, 3001 Leuven, Belgium

Electron spin resonance analysis of the intrinsic density $[P_b]$ of interfacial P_b ($\cdot Si \equiv Si_3$) defects in thermal (111)Si/SiO2 as a function of oxidation temperature T_{ox} in the range 200–1140 °C reveals a close linear correlation with the average stress σ_{av} in the superficial SiO2 layer. An almost constant high value $[P_b] \sim 1 \times 10^{13}$ cm^{-2} is found for $T_{ox} \leq 800$ °C, while from this T_{ox} onward, $[P_b]$ decreases monotonically to $< 10^{10}$ cm^{-2} along with $\sigma_{av} \to 0$ for $T_{ox} \to 1150$ °C. The underlying effect is cooperative structural relaxation of the SiO2 layer initiating at ~ 800 °C, thus gradually eliminating the need for P_b formation to account for lattice mismatch.

It has early on been recognized that, when thermally oxidizing Si, a significant number of defects are generated at the Si/SiO2 interface [1,2]. These defects have been demonstrated [3] to represent the major part—if not all—of the electrically active interface states that degrade the electrical properties of Si-based metal-oxide-semiconductor (MOS) devices. Typically an areal density of a few times 10^{12} cm^{-2} is found after clean oxidation [4] in dry O_2 at ≈ 900 °C. But it should be added in the same breath that industrial semiconductor needs have pushed the development of processing sequences that result in an effective lowering of electrically active interface defects [5] to $\approx 10^{10}$ cm^{-2}—merely realized by hydrogen passivation rather than by elimination of defect entities.

In the neutral state, these defects, labeled as P_b centers when observed by electron spin resonance (ESR) at the (111)Si/SiO2 interface, have been identified [2,4,6,7] (mainly by ESR) as a [111] sp^3-like dangling bond on an interfacial Si atom pyramidally backbonded to three Si atoms in the substrate—in shorthand denoted as $\cdot Si \equiv Si_3$. At the technologically preferred (100)Si/SiO2 interface, however, the situation is found to be more complicated as here, two variants of interface defects, labeled P_{b0} and P_{b1}, have been uncovered [7] by ESR, the atomic identification of which remains as yet unclear [8].

The P_b structure, in contrast, has apparently been well characterized. But while there is little doubt that interface mismatch, with attendant stress, governs their generation (without involvement of impurities), one is still unaware of the specific driving stress term(s)—a lacking insight that may contribute to the understanding of the P_b formation process. This particular issue is addressed in this work by combining mechanical stress and ESR data. This has been effectuated by exploring the intrinsic areal P_b density $[P_b]$ in (111)Si/SiO2, probed by ESR, as a function of oxidation temperature T_{ox} ranging from 200 up to 1140 °C. It is evident that this goal necessitates analysis of all P_b's *intrinsically* generated during thermal oxidation, as distinct from those introduced by post-oxidation damaging events, which, in addition to activation of P_b precursor sites, might also create new P_b de-

fects [9].

A key P_b feature is the dominance of its thermochemical properties by interaction with H_2. While early recognized [1,2], this aspect has recently been outlined quantitatively through detailed analysis of the H-related passivation and dissociation kinetics [10]. Passivation of P_b's was found to proceed readily in the range 230–260 °C with activation energy $E_a \sim 1.66$ eV along the reaction $Si_3 \equiv Si \cdot + H_2 \to Si_3 \equiv SiH + H$, leading to the formation of the neutral, diamagnetic (ESR-inactive) defect $HSi \equiv Si_3$, symbolized as HP_b. The dissociation step, characterized by $E_a \sim 2.56$ eV, is described by the reaction $Si_3 \equiv SiH \to Si_3 \equiv Si \cdot + H$, setting in significantly above ~ 500 °C. This (albeit often benign) H complication has crossed time and again the immense research efforts put into developing interface-state-free MOS structures. And as unintended H contamination is pervasive, it is thus not surprising to find a large spread in *as-grown* P_b density over the numerous growth facilities and procedures employed. It follows that elimination of this facility-dependent H contamination is prerequisite to a reliable ESR analysis of the intrinsically generated P_b's. This has been realized here through strict application of the previously optimized [11] reversible treatment for HP_b dissociation after each oxidation step, identically. This assures observation of the pristine density $[P_b^*]$ of intrinsically generated P_b entities at the (111)Si/SiO2 interface. Here, $[P_b^*] = [P_b] + [HP_b] + [XP_b]$, including both ESR-active (P_b) defects and centers complexed by H (HP_b) or any other means (XP_b) into a diamagnetic state. The evidence indicates that in state-of-the-art Si/SiO2 growth, $[XP_b]$ is negligible, so that, after exhaustive H liberation, $[P_b^*] = [P_b]$, the P_b density is detected by ESR.

ESR samples having a 2×9 mm^2 (111) main face were cut from a commercial Czochralski-grown p-type Si wafer (B doped, ≈ 10 Ω cm, 117 ± 16 μm thick), polished at both sides to optical finish. Prior to each oxidation, the slices were submitted to a standard RCA preoxidation cleaning, identically for all samples. Thermal oxidation was carried out in a high-vacuum laboratory setup (He leak tight to better than 10^{-10} Torr l/s) incorporat-

ing a double-walled silica tube. All oxidations occurred in flowing O_2 (99.999% pure; 1.1 atm) for 2 h, whereupon the oven was off set from the silica tube, thus allowing the samples (still in flowing O_2) to cool to room temperature (RT) in ~ 20 min. This resulted in oxide thicknesses d_{ox} ranging from ~ 115 to 2300 Å for T_{ox} varying from 800 to 1140 °C. After a first ESR diagnosis of these as-oxidized samples, they were subsequently submitted to the H-depassivation step, implying annealing in a 2×10^{-7} vacuum (turbomolecularly pumped) for 1 h at 790 ± 5 °C, again identically for all oxidation sequences. K-band (~ 20.2 GHz) ESR measurements were carried out at 4.3 K along the lines outlined elsewhere [11].

In Fig. 1(a) is plotted the variation of the intrinsic P_b density observed by ESR after exhaustive dehydrogenation as a function of T_{ox} in the range 200-1140 °C. There are two main observations pertaining to the clear division of the figure into a low- and a high-T_{ox} region, with a demarcation temperature $T_{ox}^c \approx 750$-800 °C. $[P_b]$ is seen to remain almost fixed at $\sim 1 \times 10^{13}$ cm^{-2} all over range $T_{ox} < 800$ °C, while in the high-T_{ox} region a drastic monotonic decrease with growing T_{ox} is noticed. This key observation indicates that $[P_b] \rightarrow\, < 10^{10}$ cm^{-2} (the detection limit) for $T_{ox} \rightarrow 1150$ °C.

The present correlative analysis has benefited signifi-
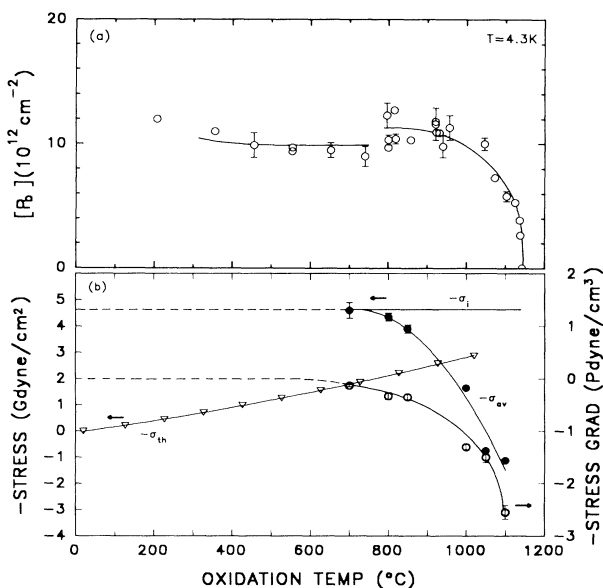
FIG. 1. (a) P_b density observed on RCA-precleaned (111)Si/SiO$_2$ (~ 1 atom dry O$_2$; 2 h) at various T_{ox} after exhaustive dehydrogenation at 790 °C for ≈ 1 h in vacuum. (b) Various stress terms identified in the superficial SiO$_2$ layer. The data points plotted for the intrinsic SiO$_2$ film stress (●) and near interfacial stress gradient (○) come from Refs. [14] and [15], where the latter values represent the slopes of the measured intrinsic stress-vs-d_{ox} curves for $d_{ox} < d_{ox}^c$ (see also Fig. 2). The solid lines through the σ_{av} and $\delta\sigma/\delta d_{ox}$ data represent least-squares parabolic fits, while the other lines are only meant to guide the eye.

cantly from previous detailed study [12-15] of stress in thermally grown SiO$_2$ on (111)Si wafers. The various stress terms so far discriminated are synopsized in Fig. 1(b). These include the following.

(1) Intrinsic interface stress σ_i, that is, the stress in the superficial SiO$_2$ film for $d_{ox} \rightarrow 0$, seen to be pinned at $\sigma_i = -4.6 \pm 0.5$ Gydn/cm^2. This large, in magnitude, stress is the embodiment of the differences in molar volume of both solids confronted at a single Si/SiO$_2$ interface plane, i.e., unequal bond length (Si-Si interatomic spacing is 2.352 and 3.06 Å in c-Si and SiO$_2$, respectively), angles, and bond densities, which prevent a perfect geometrical match.

(2) Intrinsic average stress σ_{av} developing in the thickening oxide film, where it is important to add that the data (taken from Refs. [14,15]) shown in Fig. 1(b) represent those for the oxide thicknesses actually grown (2 h) at each T_{ox} (vide infra, Fig. 2). Typifying for this stress is the fact that $|\sigma_{av}|$ ($= |\sigma_i|$ for $T_{ox} < 700$ °C) declines steadily with increasing T_{ox} above 700 °C. This behavior is clearly associated with the actual oxide thickness reached after 2 h at each T_{ox}, substantial oxidation effectively starting only above [16] T_{ox}^c. This correlation is explained by the fact that as the SiO$_2$ film grows by consumption of the Si substrate, part of the initially generated interface stress is relieved into the bulk of the oxide layer by viscoelastic motion [12,14,15,17] of SiO$_2$ away from the interface, resulting in reduced average stress. The effect is observed to accelerate drastically with increasing T_{ox}, the intrinsic stress apparently fully relaxing for $T_{ox} > 1140$ °C for sufficiently thick oxide films, in agreement with refractive index data [17,18]. Within the Maxwell viscoelastic model for a solid, this d_{ox}-coupled phenomenon reflects the drastic decrease in viscoelastic relaxation time with increasing T_{ox}. Apparently, no such relaxation can occur for $T_{ox} < 700$ °C.

(3) Thermal expansion stress, σ_{th}, which, while being zero at the actual temperature of oxidation, develops upon cooling to RT as a result of the difference in thermal expansion coefficient α between a-SiO$_2$ [$\alpha_{SiO_2} = (0.50 \pm 0.06) \times 10^{-6}$ K^{-1}, almost constant [19] within the range 300-800 °C] and Si (α_{Si} increases monotonically [20] from 2.555×10^{-6} K^{-1} at 293 K to 4.41×10^{-6} K^{-1} at 1000 K). The plotted values, well in line with experimental data, were calculated from the expression

$$\sigma_{th} = E_{ox}' \left[\alpha_{ox}(T_{ox} - 293) - \int_{293}^{T_{ox}} \alpha_{Si}(T) dT \right]. \qquad (1)$$

Here, $E_{ox}' = E_{ox}/(1 - \mu_{ox}) = 8.0 \times 10^{11}$ dyn/cm^2 is the generalized effective in-plane stress modulus, where E_{ox} and μ_{ox} represent Young's modulus and the Poisson ratio, respectively. Regarding the impact of σ_{th} on P_b generation, it should be added that, although as yet not separated, some information may be inferred from earlier work. One piece of information comes from the ESR observation of large P_b densities ($> 10^{12}$ cm^{-2}) in (111)Si/SiO$_2$ native oxide structures [21], suggesting the predominance

of intrinsic rather than thermal stress. Other evidence is provided by the ESR observation [22,23], indicating that $[P_b]$, unlike σ_{th}, remains unaltered in the range 4.2–300 K. We finally add that all three stress terms so far discussed are compressive (negative) and lateral, the stress in the perpendicular direction being small.

Also included in Fig. 1(b) are values of the intrinsic stress gradient in SiO_2 layers next to the Si/SiO_2 interface, as inferred from laser beam deflection data [14,15]. This apparently large gradient for high T_{ox} has been ascribed [15,17] to the unequal thermal history of the various oxide layers, simply referring to the fact that SiO_2 layers more remote from the interface have benefited progressively longer from stress relaxing annealing at the particular T_{ox}. Interesting is that $\delta\sigma/\delta d_{ox}$ (a positive quantity), in concert with $|\sigma_{av}|$, declines sharply above $T_{ox} > 800\,°C$. The significance of this, particularly in relation with P_b properties, may perhaps best be appreciated from Fig. 2, reproducing two intrinsic stress versus d_{ox} profiles reported in Ref. [14] for $(111)Si/SiO_2$ entities grown at 700 and 1000 °C. A key feature of this plot is the steep drop in $|\sigma_{av}|$ with increasing d_{ox}, getting steeper the higher T_{ox} and attendant with a strong *increase* in near-interfacial stress gradient. As sketched in Fig. 2, the initial drop in stress for d_{ox} smaller than a characteristic value d_{ox}^c (e.g., $d_{ox}^c \approx 22$ nm for $T_{ox} = 1000\,°C$) may be approximated by a linear relationship, the fitted lines, as expected, converging to σ_i. It is the slope of these lines for $d_{ox} < d_{ox}^c$ that is taken as a measure for the near-interface stress gradient plotted in Fig. 1(b). Figure 2 additionally illustrates that when d_{ox} exceeds d_{ox}^c, $\delta\sigma/\delta d_{ox} \rightarrow 0$, the stress levels off at a value characteristic for each T_{ox}. This amply demonstrates that, as realized in Fig. 1(b), assignment of stress must take into account the actual thickness of the grown oxide layer.

When referring to Fig. 2, it should thus not come as a surprise that the σ_{av} vs d_{ox} profile is well mirrored by the $\delta\sigma/\delta d_{ox}$ data, as shown in Fig. 1(b). At each T_{ox}, the in-

terfacial stress gradient is expected to exhibit a one-for-one relationship with the corresponding σ_{av} plateau value reached for $d_{ox} > d_{ox}^c$. And it is indeed so that for the region $T_{ox} > 800\,°C$, the presently applied 2-h oxidation time results at each T_{ox} in $d_{ox} > d_{ox}^c$, whence the close tracking.

We have now reached the point allowing us to analyze the $[P_b]$ vs T_{ox} profile in terms of stress. When first addressing the T_{ox} range above 800 °C, it is clear that neither σ_i (at least for $T_{ox} > 800\,°C$) nor σ_{th} account for the mapped T_{ox} dependence of $[P_b]$. But instead, the tracking of the $[P_b]$ data with $-\sigma_{av}$, and hence also with $-\delta\sigma/\delta d_{ox}$, appears close. The correlation between the latter quantities is borne out in Fig. 3 where $[P_b]$ is plotted versus $-\sigma_{av}$ and $-\delta\sigma/\sigma d_{ox}$ values read from the fitted curves in Fig. 1(b). Linear relationships are found (cf. Fig. 3) described by

$$[P_b](10^{12}\,\text{cm}^{-2}) = 8.27 - 0.987\sigma_{av}(\text{Gdyn/cm}^2) \quad (2)$$

and

$$[P_b](10^{12}\,\text{cm}^{-2}) = 13.3 - 0.00282\delta\sigma/\delta d_{ox}(\text{Pdyn/cm}^3)\,, \quad (3)$$

both with a correlation coefficient of 0.97. It reveals the predominant role of σ_{av} in *intrinsic* P_b formation, intimately related with the near-interfacial stress gradient [24]. This correlated decrease of σ_{av} and $[P_b]$ with growing T_{ox} above $\approx 800\,°C$, and particularly the finding that $[P_b]$ tends to vanish for $T_{ox} \rightarrow 1150\,°C$, is well in line with the SiO_2 refractive index data [18]. This index, which is accepted to be a good measure of the oxide density and stress, is seen to decrease monotonically with increasing T_{ox}, to level out at ≈ 1.460 for $T_{ox} > 1150\,°C$.

It has been concluded [25] from stress analysis on $(100)Si/SiO_2$ that there exists a correlation between the midgap interface state density D_{int} and σ_{av}. If the P_{b0} and P_{b1} defects at the (100) interface would account for

FIG. 2. Intrinsic stress in superficial SiO_2 layers on Si as measured by the laser beam deflection technique (after Ref. [14]). For each T_{ox}, the crossing of the asymptotic lines defines a characteristic thickness d_{ox}^c. Notice that an initially $(d_{ox} < d_{ox}^c)$ larger slope implies a lower stress magnitude in the thick $(d_{ox} > d_{ox}^c)$ range.
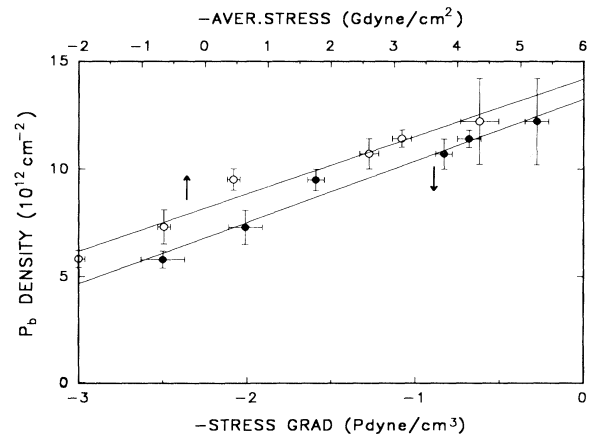
FIG. 3. Correlation of the intrinsic P_b density at $(111)Si/SiO_2$ interfaces (observed after degassing) grown in dry O_2 with stress in the SiO_2 layer for the range $T_{ox} = 800–1100\,°C$. The solid lines represent least-squares fits (cf. Refs. [2] and [3]) from where a close linear correlation is noticed.

the major part of the D_{int} states, and if assuming a similar behavior of P_{b0} and P_{b1} and P_b at the (100) and (111)Si/SiO$_2$ interfaces, respectively, the present findings corroborate the previous D_{int} results. No correlation, however, has been traced in Ref. [25] between D_{int} and the stress gradient, in contrast with the present work.

Within the framework of the mentioned viscoelastic relaxation in combination with effects imposed by different thermal history on the various layers in the oxide film, it is expected that the particular stress present in a (111)Si/SiO$_2$ structure would be the one corresponding to the highest processing temperature it has been submitted to [26], i.e., either T_{ox} or any other post-oxidation anneal temperature (evidence for this in terms of D_{int} may also be found in Refs. [13,25]). Among others, this would tell us that the intrinsic P_b density can only be significantly reduced by treatments at $T > 1100$ °C. It is recalled that we are here dealing with the *intrinsic* elimination of P_b's—not with any kind of chemical complexing of P_b's (for example, HP_b formation) leading to passivation rather than elimination of defects. The reason then why the microelectronics industry is not growing stress—and interface defect—"free" Si/SiO$_2$ is to be ascribed to the much increased risks and complications with the higher T_{ox} process, i.e., 1150 °C *vis-à-vis* the usual $T_{ox} = 800$–900 °C.

Turning to the $T_{ox} < 800$ °C range, the observation that $[P_b]$ remains almost fixed at $\sim 1 \times 10^{13}$ cm^{-2} complies with the above interpretation. It just indicates that P_b generation in this range is essentially driven by the fixed intrinsic interface stress—there exists little interfacial stress gradient within this T_{ox} range. This is also embedded in Ref. [3], showing that for $\delta\sigma/\delta d_{ox} \rightarrow 0$, the intrinsic P_b density generated is $\approx 13 \times 10^{12}$ cm^{-2}, which is to be seen as the amount generated by $\sigma_i = -4.6 \times 10^9$ dyn cm^{-2}.

In summary, strict elimination of the H passivation factor has enabled successful mapping of the *intrinsic* P_b density vs T_{ox}, revealing a close relationship of $[P_b]$ with the *average intrinsic stress* σ_{av} in the SiO$_2$ layer—not with σ_{th}. This implies that in the range below ~ 800 °C, the fixed intrinsic interface stress of ~ -4.6 Gdyn/cm^2, constituting σ_{av}, accounts for the generation of $\sim 1 \times 10^{13}$ P_b's cm^{-2}, while above 800 °C, cooperative structural relaxation of the SiO$_2$ film gradually reduces σ_{av} in the thickening SiO$_2$ with increasing T_{ox}; Eventually, $[P_b]$ tends to $< 10^{10}$ cm^{-2} for $T_{ox} \rightarrow 1150$ °C, attendant with a steep drop of the interfacial stress in the immediate oxide layers. This means tending to a complete chemical bonding at the Si/SiO$_2$ interface plane—an unattainable situation for any lower T_{ox}; it just reflects the flexibility of the amorphous SiO$_2$ structure at elevated temperatures.

[1] Y. Nishi, J. Appl. Phys. **10**, 52 (1971).

[2] P. J. Caplan, E. H. Poindexter, B. E. Deal, and R. R. Razouk, J. Appl. Phys. **50**, 5847 (1979).

[3] S. T. Chang, J. K. Wu, and S. A. Lyon, Appl. Phys. Lett. **48**, 662 (1986); G. J. Gerardi, E. H. Poindexter, P. J. Caplan, and N. M. Johnson, Appl. Phys. Lett. **49**, 348 (1986).

[4] For a recent review on Si/SiO$_2$ defect physics, see the 23 papers in Semicond. Sci. Technol. **4**, 961 (1989), and references therein.

[5] See, e.g., E. A. Irene, CRC Crit. Rev. Solid State Mater. Sci. **14**, 175 (1988).

[6] K. L. Brower, Appl. Phys. Lett. **43**, 1111 (1983).

[7] E. H. Poindexter, P. J. Caplan, B. E. Deal, and R. R. Razouk, J. Appl. Phys. **52**, 879 (1981).

[8] A. H. Edwards, Phys. Rev. B **36**, 9638 (1987); J. H. Stathis and L. Dori, Appl. Phys. Lett. **58**, 1641 (1991).

[9] Y. Nishioka, Eronides F. da Silva, Jr., and T. P. Ma, Appl. Phys. Lett. **52**, 720 (1988); W. L. Warren and P. M. Lenahan, IEEE Trans. Nucl. Sci. **34**, 1355 (1987); K. L. Brower, W. K. Shubert, and C. H. Seager, J. Appl. Phys. **68**, 366 (1990).

[10] K. L. Brower, Phys. Rev. B **38**, 9657 (1988); **42**, 3444 (1990); K. L. Brower and S. M. Myers, Appl. Phys. Lett. **57**, 162 (1990).

[11] A. Stesmans and G. Van Gorp, Phys. Rev. B **42**, 3765 (1990); **45**, 4344 (1992).

[12] E. P. Eernisse, Appl. Phys. Lett. **30**, 290 (1977).

[13] E. Kobeda and E. A. Irene, J. Vac. Sci. Technol. B **5**, 15 (1987).

[14] E. Kobeda and E. A. Irene, J. Vac. Sci. Technol. B **6**, 574 (1988).

[15] J. T. Fitch, C. H. Bjorkman, G. Lucovsky, F. H. Pollak, and X. Yin, J. Vac. Sci. Technol. B **7**, 775 (1989).

[16] M. A. Hopper, R. A. Clarke, and L. Young, J. Electrochem. Soc. **122**, 1216 (1975).

[17] K. Tanighichi, M. Tanaka, and C. Hamaguchi, J. Appl. Phys. **67**, 2195 (1990).

[18] See, e.g., B. Leroy, Philos. Mag. B **55**, 159 (1987).

[19] *Handbook of Material Sciences III* (CRC Press, Boca Raton, FL, 1975), p. 123.

[20] C. A. Swenson, J. Phys. Chem. Ref. Data **12**, 179 (1983).

[21] A. Stesmans, Appl. Surf. Sci. **30**, 134 (1987).

[22] N. M. Johnson, D. K. Biegelsen, M. D. Moyer, S. T. Chang, E. H. Poindexter, and P. J. Caplan, Appl. Phys. Lett. **43**, 563 (1983).

[23] A. Stesmans, J. Braet, J. Witters, and R. F. Dekeersmaecker, Surf. Sci. **141**, 255 (1984).

[24] It is seen in Fig. 1(b) that σ_{av}, starting at -4.6 Gdyn/cm^2 (compressive stress) for $T_{ox} < 800$ °C, appears to become positive (tensile stress) above ~ 1050 °C. This, however, has arisen from overestimating (cf. Ref. [13]) the thermal stress contribution to the measured total stress, so that, in fact, no tensile stress in the oxide results. This merely absolute shift of the σ_{av} data has little impact on the presently unveiled $[P_b]$-σ_{av} relationship. Anyway, absolute shifts drop out of the stress gradient data so that the exposed linear $[P_b]$-$\delta\sigma/\delta d_{ox}$ relationship may be seen as reassuring confirmation of the linear $[P_b]$-σ_{av} correlation.

[25] C. H. Bjorkman, J. T. Fitch, and G. Lucovsky, Appl. Phys. Lett. **56**, 1983 (1990).

[26] Strong evidence for this comes from SiO$_2$ refractive index measurements. See, e.g., L. M. Landsberger and W. A. Tiller, Appl. Phys. Lett. **51**, 1418 (1987), and Ref. [17].